



## Geomagnetic activity and polar surface air temperature variability

A. Seppälä,<sup>1,2</sup> C. E. Randall,<sup>3</sup> M. A. Clilverd,<sup>1</sup> E. Rozanov,<sup>4,5</sup> and C. J. Rodger<sup>6</sup>

Received 29 December 2008; revised 23 June 2009; accepted 14 August 2009; published 21 October 2009.

[1] Here we use the ERA-40 and ECMWF operational surface level air temperature data sets from 1957 to 2006 to examine polar temperature variations during years with different levels of geomagnetic activity, as defined by the  $A_p$  index. Previous modeling work has suggested that  $\text{NO}_x$  produced at high latitudes by energetic particle precipitation can eventually lead to detectable changes in surface air temperatures (SATs). We find that during winter months, polar SATs in years with high  $A_p$  index are different than in years with low  $A_p$  index; the differences are statistically significant at the 2-sigma level and range up to about  $\pm 4.5$  K, depending on location. The temperature differences are larger when years with wintertime Sudden Stratospheric Warmings (SSWs) are excluded. We take into account solar irradiance variations, unlike previous analyses of geomagnetic effects in ERA-40 and operational data. Although we cannot conclusively show that the polar SAT patterns are physically linked by geomagnetic activity, we conclude that geomagnetic activity likely plays a role in modulating wintertime surface air temperatures. We tested our SAT results against variation in the Quasi Biennial Oscillation, the El Niño Southern Oscillation and the Southern Annular Mode. The results suggested that these were not driving the observed polar SAT variability. However, significant uncertainty is introduced by the Northern Annular Mode, and we cannot robustly exclude a chance linkage between sea surface temperature variability and geomagnetic activity.

**Citation:** Seppälä, A., C. E. Randall, M. A. Clilverd, E. Rozanov, and C. J. Rodger (2009), Geomagnetic activity and polar surface air temperature variability, *J. Geophys. Res.*, *114*, A10312, doi:10.1029/2008JA014029.

### 1. Introduction

[2] Odd nitrogen produced in the mesosphere or thermosphere by energetic particle precipitation (EPP- $\text{NO}_x$ ) can be transported to the stratosphere where it chemically perturbs ozone ( $\text{O}_3$ ) distributions [e.g., López-Puertas *et al.*, 2005; Randall *et al.*, 1998, 2001, 2005; Seppälä *et al.*, 2004, 2007]. Changes in  $\text{O}_3$  can further lead to changes in temperature and ultimately in atmospheric dynamics, both of which are important to the global climate [see, e.g., Brasseur and Solomon, 2005, chapter 4]. A chemistry-climate model study by Rozanov *et al.* [2005] examined the effect of continuous, low intensity, electron precipitation on the atmosphere. They predicted that the EPP- $\text{NO}_x$  increases would result in up to 30% annual ozone decreases in the polar stratosphere. This would lead to cooling of the polar middle stratosphere by up to 2 K, with detectable

changes in the surface air temperature (SAT). One possible mechanism connecting the EPP- $\text{NO}_x$  and the changes at surface level could be coupling through planetary wave breaking [Song and Robinson, 2004]: If the ozone changes were significant enough to affect stratospheric winds so that breaking of vertically propagating planetary-scale Rossby waves from the troposphere would be affected [Hartley *et al.*, 1998], this breaking could drive the downward propagation of Northern Annular Mode-like patterns which would ultimately be seen in the Surface Air Temperatures [Baldwin and Dunkerton, 1999]. Model results are in deed showing increasing evidence that stratospheric processes are able to affect surface level climate: Turner *et al.* [2009] suggest that stratospheric ozone levels are likely effecting sea ice extent trends in the Southern polar region. The results of Rozanov *et al.* [2005] indicate that the magnitude of the atmospheric response from EPP could potentially exceed the effects arising from variations of solar UV flux. In this paper, we test the validity of the model results by comparing observed mid-high latitude SATs in years with differing levels of geomagnetic activity.

[3] Previous observational investigations of the relationship between geomagnetic activity and climate are inconclusive as to the role of EPP- $\text{NO}_x$ . Boberg and Lundstedt [2002] found a correlation between the solar wind and the North Atlantic Oscillation (NAO) index [e.g., Hurrell *et al.*, 2003]. In accordance with recent practice, we hereinafter use the term Northern Annular Mode (NAM) to refer to this mode of atmospheric variability, in which the surface pressure resembles an annulus, with a large negative center

<sup>1</sup>Physical Sciences Division, British Antarctic Survey (NERC), Cambridge, UK.

<sup>2</sup>Also at Earth Observation, Finnish Meteorological Institute, Helsinki, Finland.

<sup>3</sup>Laboratory for Atmospheric and Space Physics and Department of Atmospheric and Oceanic Sciences, University of Colorado, Boulder, Colorado, USA.

<sup>4</sup>Physical-Meteorological Observatory/World Radiation Center, Davos, Switzerland.

<sup>5</sup>Institute for Atmospheric and Climate Science, Eidgenössische Technische Hochschule, Zurich, Switzerland.

<sup>6</sup>Department of Physics, University of Otago, Dunedin, New Zealand.

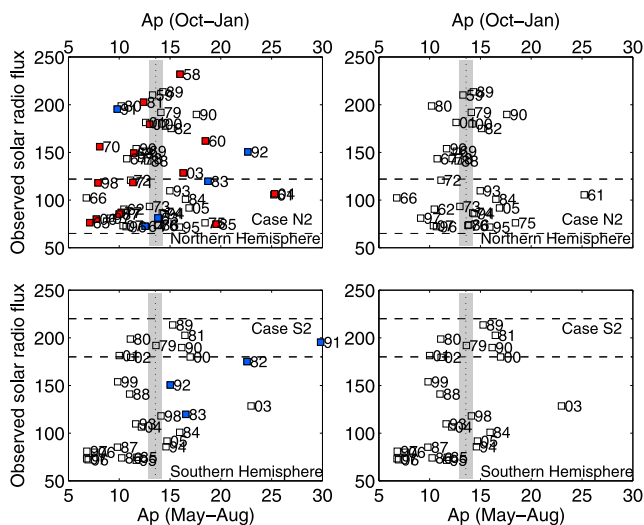


**Figure 1.** Wintertime average  $A_p$  index (October–January for NH and May–August for SH) and observed solar radio flux. (top) Northern Hemisphere, years 1958–2007. (bottom) Southern hemisphere, years 1979–2007. Years potentially affected by volcanic eruptions are marked with blue color. Years when a sudden stratospheric warming occurred in November–January are marked with red color. The horizontal dashed lines indicate Case N2 and S2 F10.7 limits. The dotted vertical line with underlying shaded gray area marks the mean  $A_p \pm 5\%$ .

over the pole and two positive centers at lower latitudes over the Atlantic and Pacific. *Boberg and Lundstedt* [2002] attributed this correlation to the influence on the troposphere of a change in geomagnetic activity caused by a solar wind-induced change to the ionospheric global electric circuit. They did not, however, relate the geomagnetic activity to EPP. *Thejll et al.* [2003] found significant correlations in the northern hemisphere (NH) wintertime between the  $A_p$  geomagnetic activity index and the NAM from 1973 to 2000, but did not account for solar irradiance variations that might have affected the correlations. *Lu et al.* [2008] showed statistically significant correlations between the  $A_p$  index and stratospheric circulation during spring that descended in altitude from month to month, but suggested that these were inconsistent with an EPP- $\text{NO}_x$  mechanism. *Langematz et al.* [2005] incorporated an idealized EPP- $\text{NO}_x$  source in their climate model and found that once transported to the stratosphere, the EPP- $\text{NO}_x$  modified the ozone response to the 11-year solar irradiance cycle. Their model results revealed a positive dipole upper stratospheric ozone signal at high latitudes, but also indicated a negative ozone signal at equatorial latitudes, where the simulated EPP- $\text{NO}_x$  levels were overestimated, compared with observations. Recently *Austin et al.* [2008] studied the 11-year solar cycles in ozone and temperature using several coupled chemistry climate models. Among other things, they considered the importance of upper atmospheric effects and concluded that, unlike the results of *Langematz et al.* [2005], EPP- $\text{NO}_x$  was not required to simulate the tropical ozone signal.

[4] According to the Intergovernmental Panel on Climate Change [IPCC, 2007] “More research to investigate the effects of solar behavior on climate is needed before the

magnitude of solar effects on climate can be stated with certainty.” While the IPCC focuses on the effects of changing solar irradiance, they also note that there might be other mechanisms through which the Sun can couple to the Earth’s climate [IPCC, 2007, Chapter 1]. In this paper we utilize meteorological analyses to investigate the possible influence of variations in geomagnetic activity on SATs in both hemispheres; we control for solar irradiance variability and discuss other possible sources of variability that might also affect SATs.

## 2. Description of Data and Method

[5] The European Centre for Medium-Range Weather Forecast (ECMWF) ERA-40 data set, described in detail by *Uppala et al.* [2005], is a reanalysis of meteorological observations extending from September 1957 to August 2002. The data set is not recommended for SH use prior to 1979 due to a lack of observational data, so our SH ERA-40 analysis is limited to the years 1979–2002. To extend our analysis beyond 2002 we utilize operational meteorological data also provided by the ECMWF. The operational data used here covers the period from 2002 to January 2007. The combination of these two data sets will be henceforth referred to as extended ERA-40. For our SAT analysis we use the air temperature at ground level, on a horizontal grid of  $2.5^\circ$  (lat) and  $5^\circ$  (lon).

[6] The atmosphere is affected by several different types of particle precipitation. This includes both electron and proton precipitation, and the sources can vary over a wide range of energies from high energy particles from the Sun (e.g., Solar Proton Events) to auroral energy precipitation. To incorporate such a wide range of particle energies in our analysis, we have chosen to use the geomagnetic activity index  $A_p$  [Mayaud, 1980] as a proxy for the overall EPP level, although the amount of EPP- $\text{NO}_x$  reaching the stratosphere will also be modulated by the prevailing meteorological conditions [Randall et al., 2006]. While there appear to be highly sufficient climatologies of low energy electrons ( $<20$  keV), and direct observations of solar proton events since the late 1970s, there is currently insufficient knowledge concerning the precipitation of medium and high energy ( $>20$  keV) electrons into the atmosphere to enable the kind of analysis we describe in this study using the extended ERA-40 data set. To account for the time taken for the EPP- $\text{NO}_x$ , originally produced in the mesosphere or thermosphere, to descend to the stratosphere, we average the  $A_p$  values over a 4-month period starting two months prior to the surface air temperature examination months [e.g., *Siskind et al.*, 2000; *Seppälä et al.*, 2007]. Using 4 month averages for  $A_p$  and 3 months for the temperature with a time lag of 2 months for the delays caused by the descent of  $\text{NO}_x$ , while the overlapping time windows take into account mechanisms that could link  $A_p$  and SAT more rapidly. To test for variations caused by solar irradiance changes, we will also undertake some analysis by subdividing the average wintertime  $A_p$  index according to the annual average solar radio flux at 10.7 cm (F10.7, [ $10^{-22}$  W m $^{-2}$  Hz $^{-1}$ ]), commonly used to indicate the solar cycle phase. The SAT results presented in the next section were similar whether an annual average or shorter (DJF) F10.7 was used.

**Table 1.** Conditions of the Different Cases<sup>a</sup>

Case	NH/SH	Solar Cycle (F10.7)	High $A_p$ Years <sup>b</sup>	Low $A_p$ Years <sup>b</sup>
N1	NH	All	1958, 1960, 1961, 1975, 1982, 1984, 1985, 1989, 1990, 1993, 1994, 1995, 2003, 2004, 2005	1962, 1965, 1966, 1967, 1968, 1969, 1970, 1971, 1972, 1977, 1978, 1980, 1981, 1987, 1988, 1991, 1996, 1997, 1998, 1999, 2001, 2002, 2006
N2	NH	Low (65–120)	1961, 1974, 1975, 1985, 1994, 1995, 2004, 2005	1962, 1965, 1966, 1971, 1972, 1977, 1987, 1996, 1997, 1998, 2006
S1	SH	All	1981, 1989, 1990, 1994, 2000, 2003, 2005	1980, 1985, 1986, 1987, 1988, 1995, 1996, 1997, 1999, 2001, 2002, 2004
S2	SH	High (180–220)	1981, 1989, 1990, 2000	1979, 1980, 2001, 2002

<sup>a</sup>Note that in this table SSW years (see Figure 1) are included.

<sup>b</sup>NH winters are referred to as 1961 for 1960/1961, etc.

[7] Figure 1 compares the  $A_p$  index to the F10.7 flux in the NH (top) and SH (bottom). The panels on the left show all the years, including those years which will be excluded in the following analysis in some cases. Years which have possible affects from volcanic eruptions are shown in blue, and are always excluded from our subsequent analysis. In addition, years when a major Sudden Stratospheric Warming (SSW [Kuroda, 2008]) occurred in the NH during the winter season (November–January) are shown in red [see, e.g., Manney *et al.*, 2005]. We will investigate the effect of these SSWs to the results. We note here that, according to Figure 1, there appears to be no relation between the SSW occurrence and  $A_p$ . In the SH, there are no known SSWs during the winter season (June–August) and thus we do not consider the SH SSW further. The panels on the right show the remaining years after the volcanic and SSW cases are excluded. As a first test we simply group the years into high and low  $A_p$  regimes according to the average  $A_p \pm 5\%$  as shown in Figure 1. We call these Case N1 (11 years of high  $A_p$ , 13 years of low  $A_p$ ) and S1 (8 years of high  $A_p$ , 15 years of low  $A_p$ ) for the NH and SH respectively. Further, to control for solar irradiance variations over the solar cycle, we selected a subset of only years with low F10.7 values (65–120, Case N2, NH), and high (180–220, Case S2, SH) F10.7 values. These subsets are selected so that they have as large variation of the  $A_p$ , with respect to the average  $A_p$  shown in Figure 1, as possible. For each case this resulted in representatively high and low  $A_p$  values for a limited F10.7 solar irradiance variation. The corresponding years for high (low)  $A_p$  are 1961, 1974, 1975, 1985, 1994, 1995, 2004,

2005 (1962, 1965, 1966, 1971, 1972, 1977, 1987, 1996, 1997, 1998, 2006) for Case N2; and 1981, 1989, 1990, 2000 (1979, 1980, 2001, 2002) for Case S2. Note that NH winters are referred to as 1961 for 1960/1961, etc. Details of the different cases mentioned above are given in Table 1. The F10.7 flux grouping could be different for the two hemispheres as it is not critical for our analysis to select the years from a particular solar cycle phase, as long as the F10.7 is limited to minimize the solar cycle induced variation in the SATs. The reason for selecting low F10.7 years in the NH case N2 and high F10.7 years in the SH case S2 is that with these F10.7 value limitations we are able to have as much deviation for the  $A_p$  values (between low and high  $A_p$  years) as possible, while at the same time having as large number of years above and below the average  $A_p$  as possible, this holding also after SSW and volcanic years have been removed.

### 3. Results

[8] Figure 2 shows the Case N1 differences ( $\Delta T$ ) between the seasonally (DJF, MAM, JJA, SON) averaged SATs for the high  $A_p$  minus low  $A_p$  years, when the SSW years are included. Note that to aid comparison of the following figures (Figures 2–7, 9, 10) we have used identical color palette scalings (from  $-5$  K to  $+5$  K) for all of the maps. In Figure 3 we repeat the analysis but have excluded the major SSW years as shown in Figure 1 (top right), as major SSWs are known to affect the tropospheric climate [see, e.g., Kuroda, 2008, and references therein]. We calculated confidence levels for each case using the

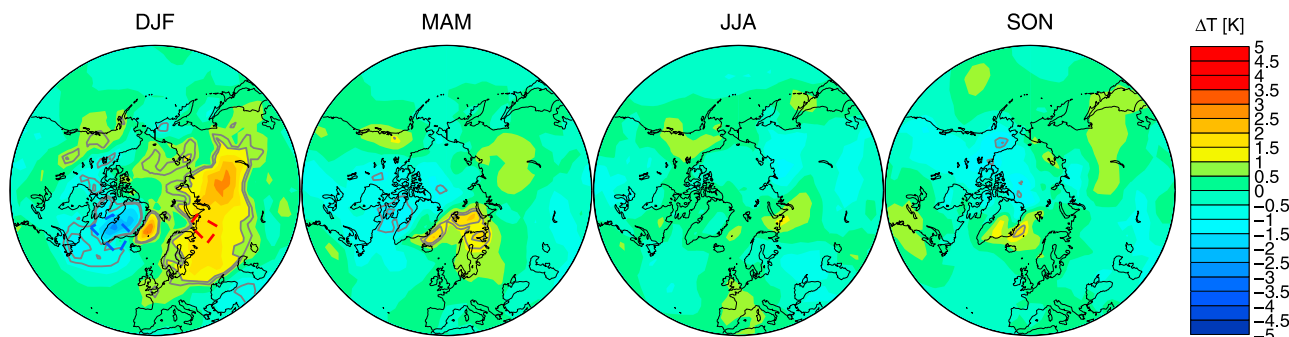


**Figure 2.** Northern hemisphere seasonal differences in SAT ( $\Delta T = \text{High } A_p - \text{Low } A_p$ ) for Case N1 with SSW years included for the seasons denoted in each column. White contours in this and the following figures represent the 90% and 95% confidence levels. The red and blue dashed boxes plotted over the DJF SAT differences indicate the regions used in the analysis presented in Figure 8.

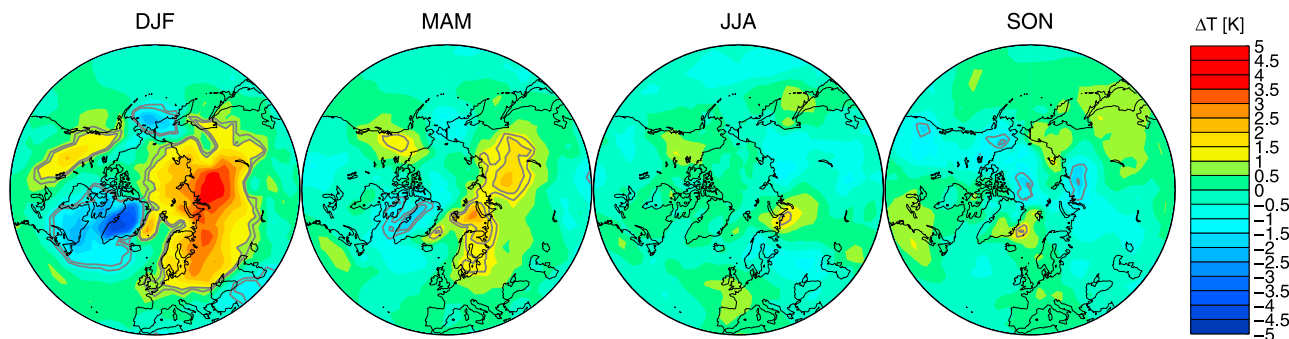


**Figure 3.** Northern hemisphere seasonal differences in SAT ( $\Delta T = \text{High } A_p - \text{Low } A_p$ ) for Case N1 with SSW years excluded for the seasons denoted.

Student  $t$ -test. The 90% and 95% confidence levels are shown in the  $\Delta\text{SAT}$  figures. Both Figures show similar DJF  $\Delta\text{SAT}$  patterns, with warming over the Northern Eurasian continent and cooling over the Greenland area. When the SSW years were excluded the statistically significant areas increased and the temperature variability increased to  $-4.5$  K over Greenland and to 4 K over Northern Eurasia.

[9] Figures 4 and 5 show the Case N2 (controlled for solar irradiance variation) differences ( $\Delta\text{SAT}$ ) between the seasonally averaged SATs for the high  $A_p$  minus low  $A_p$  years with and without the SSW years, respectively. As in Case N1, Case N2 in DJF shows warming over the Eurasian continent and northern North America, and the patterns extend in area and become somewhat more intense when SSWs are excluded. This might be as a result of more stable vortex conditions aiding downward propagation of the signals. The alternating cooling/warming pattern seen in Figures 2–5 resembles the model results of *Rozanov et al.* [2005], who suggest that it is typical for enhanced EPP- $\text{NO}_x$  in the presence of enhanced polar vortex intensity. Similar structure in the surface level temperature anomaly is observed for the wintertime Northern Annular Mode (NAM) [e.g., see Figure 13 in *Hurrell et al.*, 2003], suggesting that variations in the  $A_p$  may modulate the preexisting NAM. The pattern seen in DJF appears to subside during the spring months and disappears by summer (JJA). For Case N2 a new pattern begins to emerge again in SON, which in these seasonal averages has little resemblance to the DJF patterns.

It should be noted, however, that monthly averages (not shown because of their lower statistical significance) show large regions where  $\Delta\text{SAT}$  approaches  $\pm 4$  K in October and November, with the Case N2 pattern in November being very similar to December, but offset in location. This suggests that the physical mechanism responsible for the DJF differences could have started as early as October.

[10] Figures 6 and 7 are analogous to Figures 3 and 5, but for the southern hemisphere Cases S1 and S2. As in Cases N1 and N2, there are alternating patterns of warming and cooling in wintertime (JJA)  $\Delta\text{SAT}$ ; there is also substantial cooling in the fall (MAM). The maximum JJA  $\Delta\text{SAT}$  is  $\sim 5$  K in the western part of the Antarctic region, in the Antarctic Peninsula and the Amundsen Sea. The JJA  $\Delta\text{SAT}$  pattern is somewhat similar to the Southern Annular Mode (SAM) in terms of warming ( $< 1$  K) in the Antarctic Peninsula region, but inconsistent with SAM-induced cooling elsewhere over the continent [Thompson and Wallace, 2000]. The cooling over the continent observed in the fall (MAM) is more consistent with the SAM pattern.

[11] Next we compare the year-to-year SAT variability in specific regions directly with  $A_p$  variability; although, due to the complexity of atmospheric processes one would not expect any connection between geomagnetic activity and the surface temperature variability to necessarily be the most dominant influence from year-to-year. This is one of our main reasons for attempting to do a statistical study. For the comparison of the temporal variability of the SAT and

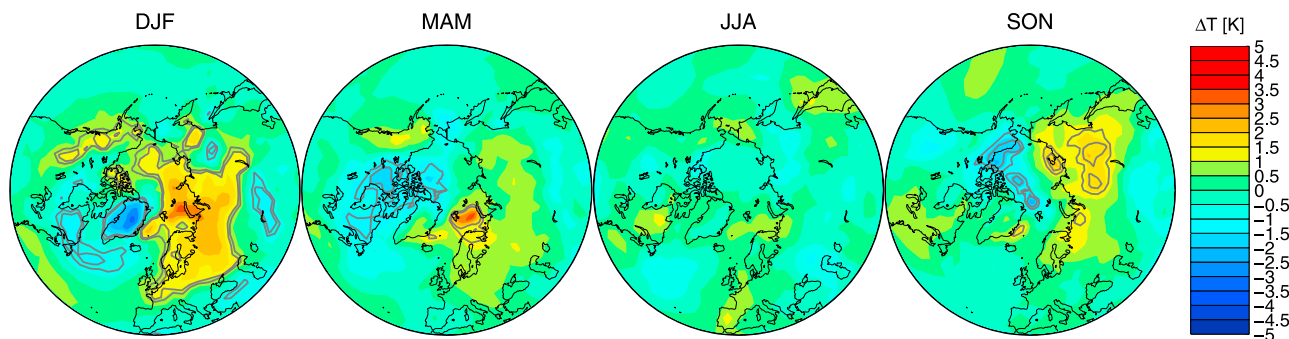


**Figure 4.** Northern hemisphere seasonal differences in SAT ( $\Delta T = \text{High } A_p - \text{Low } A_p$ ) for Case N2, which has low F10.7, i.e., removing solar cycle variations. SSW years included.



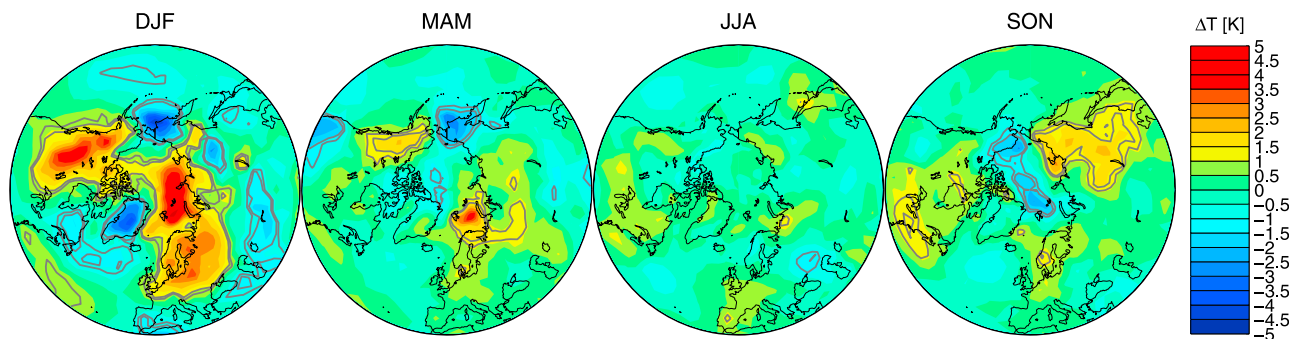


**Figure 5.** Northern hemisphere seasonal differences in SAT ( $\Delta T = \text{High } A_p - \text{Low } A_p$ ) for Case N2, no SSW years included.

the  $A_p$  we select two regions in the NH based on the DJF warm-cool regional patterns in Figures 2 and 3. The first region is that between latitudes  $60^\circ\text{N}$ – $70^\circ\text{N}$  and longitudes  $45^\circ\text{E}$ – $60^\circ\text{E}$  (corresponding to positive  $\Delta\text{SAT}$  region shown as a red dashed box in Figures 2 and 3) and the second region between latitudes  $60^\circ\text{N}$ – $70^\circ\text{N}$  and longitudes  $60^\circ\text{W}$ – $30^\circ\text{W}$  (corresponding to negative  $\Delta\text{SAT}$  region shown as a blue dashed box in Figures 2 and 3). The correlation plots for the two regions are shown in Figure 8. The panels on the left present the correlation of the values with  $A_p$  on the  $x$  axis and the SAT values on the  $y$  axis and the panels on the right present the year-to-year variability of both parameters. The panels on the right show the DJF SAT and the ONDJ  $A_p$  as a function of time to allow a better visualization of the year-to-year variability of these two parameters. The top panels correspond to the positive region and the bottom panels to the negative region in Figures 2 and 3. Volcanic and SSW years are indicated (left) with color as before. For the positive region the correlation for all years is  $\sim 0.30$ . When volcanic and SSW years are excluded the correlation increases slightly to  $\sim 0.45$ . For the negative region we find that the correlation for all years is weakly negative at  $\sim -0.20$  increasing slightly to  $\sim -0.32$  with the exclusion of volcanic and SSW years. The correlation increasing slightly with the exclusion of volcanic and SSW years might reflect the exclusion of the SSW years leading to inclusion of years with more stable polar vortex; This could potentially affect the probability of any signals originating from higher altitudes reaching the surface level.

[12] We further examined the consistency of NH DJF  $\Delta\text{SAT}$  patterns using daily ground station SAT measure-

ments [see Klein Tank *et al.*, 2002]. Nine ground stations located in Greenland, Norway, and Finland were selected. The Greenland stations were located in the area of negative extended ERA-40  $\Delta\text{SAT}$  in DJF shown in Figure 3, while the stations in Norway and Finland were located in the area of positive  $\Delta\text{SAT}$  as seen in Figure 5. Table 2 gives the average ground station temperatures and  $\Delta\text{SAT}$  (high  $A_p$  minus low  $A_p$ ) for DJF of both Case N1 and Case N2 years. Consistent with the extended ERA-40 shown in Figures 2–5, ground station  $\Delta\text{SAT}$  is negative for Greenland and positive elsewhere, the Finland stations having a high statistical significance. The results indicate low statistical significance for Greenland in Case N2 and Norway in Case N1. This would appear to agree with Figures 5 and 3, respectively, which show that these regions have  $\Delta\text{SAT}$  close to 0 K with low statistical significance. These results from the ground stations' data indicate that the NH DJF  $\Delta\text{SAT}$  patterns are likely not artifacts of the ERA-40 reanalysis data set.

[13] As a further extended ERA-40 consistency check, we repeated the SAT analysis using the National Center for Environmental Prediction (NCEP) data set; we find that the  $\Delta\text{SAT}$  patterns from the NCEP analysis agree with the extended ERA-40 data (not shown).

## 4. Discussion

### 4.1. Atmospheric Variability

[14] Attribution of  $\Delta\text{SAT}$  patterns to geomagnetic activity variations requires ruling out other sources of variability. In the analysis presented above we focused on minimizing

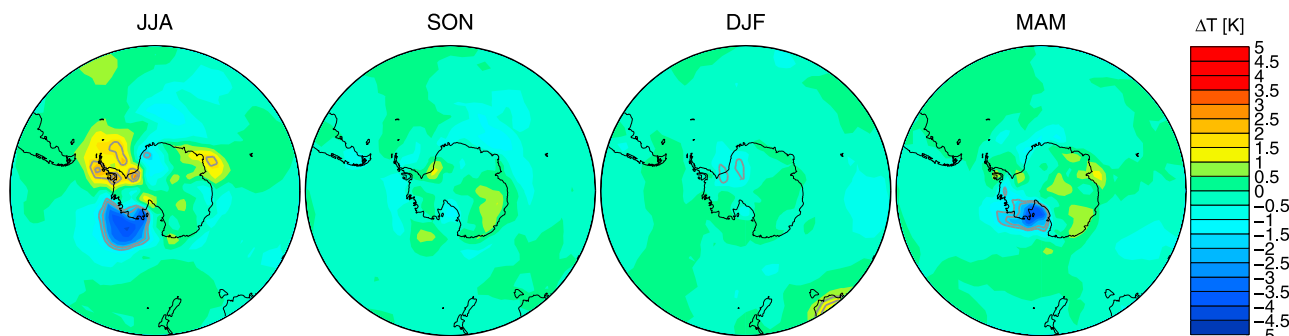


**Figure 6.** Southern hemisphere seasonal differences in SAT ( $\Delta T = \text{High } A_p - \text{Low } A_p$ ) for Case S1.

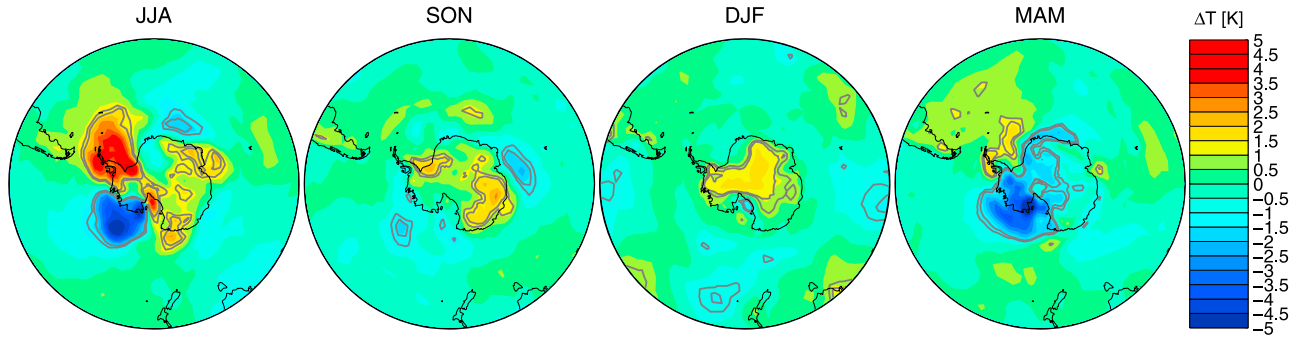


**Figure 7.** Southern hemisphere seasonal differences in SAT ( $\Delta T = \text{High } A_p - \text{Low } A_p$ ) for Case S2.

solar irradiance variability effects by subsampling the extended ERA-40 data according to the F10.7 flux. We also considered the effects of major SSWs and volcanic eruptions. Here we consider four other processes: the Quasi Biennial Oscillation (QBO), the El Niño Southern Oscillation (ENSO), NAM, and SAM. We have also considered the possibility that our results could be affected by slow variations in Sea Surface Temperatures (SST) influencing tropospheric temperatures and that there might be a random correlation between the SST and geomagnetic activity. However, determining SST effects on the  $\Delta SATs$  discussed in this paper is a complicated task and therefore we will not consider any possible SST effect further, but will be mindful of it.

[15] Since large  $\Delta SAT$  values were found in winter months in both hemispheres, we focus on winter. To account for possible time lags, we compared indices for these sources of atmospheric variation during high- and low- $A_p$  years averaged in 3-month increments during the months of October–February for NH Cases N1 and N2, and April–August for SH Cases S1 and S2. The results of this comparison are presented in Table 3. To put the differences into context, Table 3 also gives the minimum, maximum, and standard deviation ( $\sigma$ ) of each index from 1950 to 2007.

[16] The results in Table 3 suggest that the QBO, ENSO, and SAM are not primarily responsible for the differences seen in Figures 3 and 5–7. In all but one of these cases, the index differences are significantly less than  $\sigma$ . The one

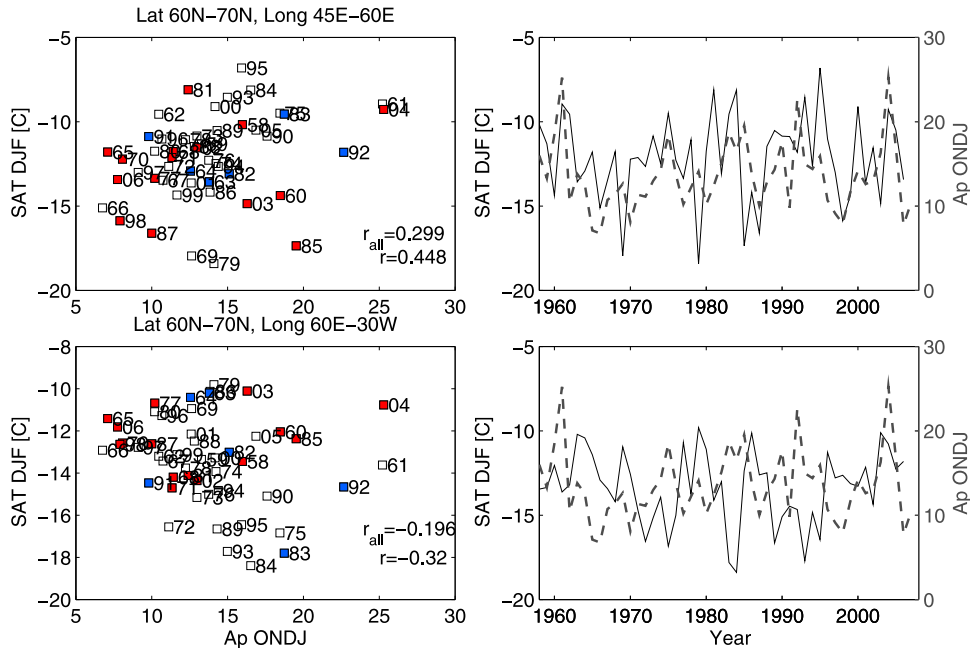


**Figure 8.** (left)  $A_p$  (October–January) SAT (December–February) correlation from the ERA-40 reanalysis. Years with Sudden Stratospheric Warmings occurring in November–January are shown in red color, and years following major volcanic eruptions are shown in blue. The top row corresponds to the area limited by latitudes 60°N and 70°N and longitudes 45°E and 60°E, and the bottom row to the area limited by latitudes 60°N and 70°N and longitudes 60°E and 30°W (as shown in Figure 2). Correlation coefficients are calculated including all data points ( $r_{all}$ ) and also excluding SSW and volcanic years ( $r$ ). (right) Corresponding SAT (solid line) and  $A_p$  (dashed line) time series. Note: Volcanic and SSW years are plotted in this time series.

**Table 2.** Ground Station DJF Average Temperatures During High (Low)  $A_p$  Years for Cases N1 and N2<sup>a</sup>

Location	DJF Temperature for High (Low) $A_p$		$\Delta$ SAT (Confidence Level)	
	Case N1 <sup>b</sup>	Case N2 <sup>c</sup>	Case N1 <sup>b</sup>	Case N2 <sup>c</sup>
Greenland <sup>d</sup>	−10.5 (−8.9)	−9.4 (−9.3)	−1.6 (85%)	−0.1 (3%)
Norway <sup>e</sup>	−10.4 (−10.5)	−8.3 (−11.3)	0.1 (7.3%)	3.0 (86%)
Finland <sup>f</sup>	−13.8 (−11.1)	−10.2 (−14.4)	2.7 (97%)	4.2 (98%)

<sup>a</sup>The last two columns show  $\Delta$ SAT, with the confidence level given in parentheses. Data and metadata available at <http://eca.knmi.nl>; see Klein Tank *et al.* [2002].

<sup>b</sup>Case N1 with SSW years excluded.

<sup>c</sup>Case N2 with SSW years excluded.

<sup>d</sup>Ilulissat (69°13′, −51°6′), Tasillaq (65°36′, −37°38′).

<sup>e</sup>Bjoernoeya (74°31′, 19°1′), Svalbard (78°15′, 15°28′), Hopen (76°30′, 25°4′), Glomfjord (66°49′, 13°59′), Karasjok (69°28′, 25°31′), Vardoe (70°22′, 31°5′), 31°5′).

<sup>f</sup>Sodankylä (67°22′, 26°39′).

exception is the QBO for Case S1, where the differences (AMJ, MJJ, JJA) approach  $\sigma$ . In this case, however the Case S1 difference is opposite in sign to Case S2; that the  $\Delta$ SAT patterns for Cases S1 and S2 are similar suggests, therefore, that QBO variations are not the cause of these patterns.

[17] The situation is more complex for the NAM. The NAM index difference is on the order of  $\sigma$  in all 3-month averages except OND in Case N1 and N2. In all cases, the NAM index differences are positive, indicating that  $\Delta$ SAT values in Figures 3 and 5 would take on characteristics of the positive NAM phase. In the positive NAM phase, Greenland tends to be cooler and northern Eurasia warmer than otherwise. It should be noted here that, unlike NAM geopotential and zonal wind patterns, the NAM SAT pattern is not zonally symmetric [Thompson and Wallace, 2000; Hurrell *et al.*, 2003]. This is consistent with the DJF  $\Delta$ SAT patterns seen in Figures 3 and 5. Hurrell *et al.* [2003] show warming (cooling) of up to about 2 K (1.4 K) in northern Eurasia (near Greenland) for a one-unit increase in the NAM index during December–March. Maximum DJF  $\Delta$ SAT values in Figure 5 are about twice this size for both Cases 1 and 2. Attributing the observed  $\Delta$ SAT values to the NAM requires that  $\pm 4$  K changes result from index changes of  $\sim 1$ ; such changes are not ruled out by Hurrell *et al.* [2003], since their  $\sim 2$  K changes represented averages over years 1900–2002.

#### 4.2. Temperature Variability Tests

[18] Here we examine the possibility that the observed  $\Delta$ SAT patterns in the NH and SH could simply be formed randomly. We do this by selecting the sets of years, for which

the  $\Delta$ SAT are calculated, using different,  $A_p$ -independent criteria.

[19] First we test the consistency of the patterns seen in Figures 2–5 by grouping the NH years according to the F10.7 flux and calculating the difference between years with higher and lower F10.7 values. The higher value years are defined as those with F10.7 > 150 and the lower value years as those with F10.7 < 150. Figure 9 presents the NH seasonal SAT differences when SSW years were excluded. The main features in Figure 9 are a DJF warm pattern in midlatitude Eurasia and North America and Greenland and a cool pattern in Northern Eurasia. Other seasons do not show statistically significant patterns. When Figure 9 is compared with the earlier Figure 3, it is evident that the temperature variability patterns differ, and that the temperature range in Figure 3 is nearly twice that of Figure 9. This suggests that the SAT variability patterns of Figure 3 are not induced by the variability in solar flux, caused by the 11-year solar cycle.

[20] As can be seen from Figure 1 (left), in the SH the solar F10.7 radio flux *i.e.* the solar cycle phase and the geomagnetic activity index  $A_p$  are slightly more correlated than in the NH, in the sense that in the SH the lowest  $A_p$  values correspond to low F10.7 values. Thus simply grouping the SH years according to the F10.7 as we did for the NH would not provide an  $A_p$ -independent test. As a test of the SH temperature variability pattern we therefore imposed a linear division of all the years from low  $A_p$ -low F10.7 to high  $A_p$ -high F10.7. This divides all SH years into two groups, one group including 1980, 2001, 2002, etc., and the other group including 1994, 1995, 2005, etc. The seasonal

**Table 3.** Oscillation Index Tests<sup>a</sup>

Index	OND		NDJ		DJF		AMJ		MJJ		JJA		Max/Min/ $\sigma$
	N1	N2	N1	N2	N1	N2	S1	S2	S1	S2	S1	S2	
QBO <sup>b</sup>	−3.50	−0.58	−3.38	−1.50	−3.81	−2.28	−9.02	4.75	−11.94	3.61	−14.27	1.46	15.62/−29.55/11.11
ENSO <sup>c</sup>	−0.01	0.03	−0.03	−0.13	0.04	−0.13	−0.24	−0.60	−0.36	−0.65	−0.38	−0.72	3.15/−2.25/0.97
NAM <sup>d</sup>	0.28	0.44	0.84	0.98	0.83	0.83	—	—	—	—	—	—	3.04/−3.18/0.99
SAM <sup>e</sup>	—	—	—	—	—	—	0.03	0.23	0.21	0.51	0.15	−0.10	2.69/−3.01/0.99

<sup>a</sup>Columns OND through JJA give 3-month averages of high  $A_p$  minus low  $A_p$  differences for each index shown for Cases N1, N2, S1 and S2; e.g., OND means October–November–December; JJA means June–July–August, etc. The QBO index row shows the differences in equatorial zonal wind speeds. The last three columns give the maximum, minimum and standard deviation of each index from 1950 to 2007. Note that NAM (SAM) indices are not calculated for the Northern (Southern) summer months AMJJA (ONDJF).

<sup>b</sup><http://www.cdc.noaa.gov/Correlation/qbo.data>.

<sup>c</sup>Multivariate ENSO Index: <http://www.cdc.noaa.gov/people/klaus.wolter/MEI/table.html>.

<sup>d</sup><http://www.cpc.noaa.gov/products/precip/CWlink/pna/norm.nao.monthly.b5001.current.ascii.table>.

<sup>e</sup>[http://www.cpc.noaa.gov/products/precip/CWlink/daily\\_ao\\_index/ao/monthly.ao.index.b79.current.ascii.table](http://www.cpc.noaa.gov/products/precip/CWlink/daily_ao_index/ao/monthly.ao.index.b79.current.ascii.table).

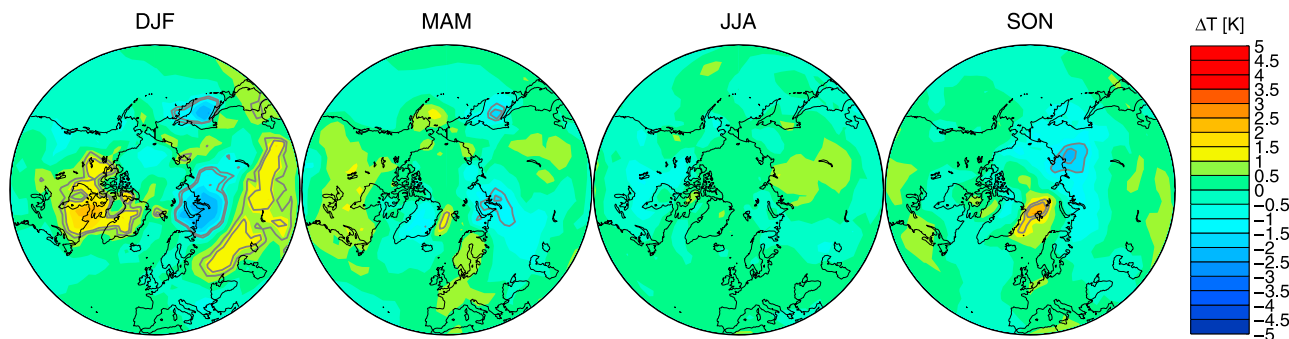


**Figure 9.** Northern hemisphere high solar years ( $F_{10.7} > 150$ ) – Low solar years ( $F_{10.7} < 150$ ), no SSW years included.

SAT differences of these two groups are presented in Figure 10. This Figure 10 is to be contrasted with Figures 6 and 7 showing the High – Low  $A_p$  index patterns. Figure 10 JJA shows a weak ( $< 1.5$  K) warming pattern placed between the warm and cool patterns of Figures 6 and 7. As in the NH, the magnitude of the JJA SAT variability ( $-2$  to  $1.5$  K) is smaller than for the High – Low  $A_p$  (up to  $-5$  to  $5$  K). This would suggest that the SAT variability patterns of Figures 6 and 7 are not induced by random variability in solar flux and the  $A_p$ .

## 5. Summary

[21] Using the ERA-40 data set from 1957 to 2002 and ECMWF operational meteorological data from 2002 onward, we find statistically significant differences in wintertime polar SAT between years with high and low  $A_p$  index. The changes occur in both hemispheres and are on the order of  $\pm 4.5$  K. In the NH the changes are more evident when years with Sudden Stratospheric Warmings occurring during the midwinter months are excluded from the analysis. These results agree with previous model predictions of EPP effects in the lower atmosphere [Rozanov *et al.*, 2005]. We conclude that geomagnetic activity is a likely cause of the SAT changes, although possible effects from the NAM introduce a high level of uncertainty in this conclusion. Random sources of atmospheric variability that are not quantified by the indices evaluated here (QBO, ENSO, NAM and SAM) can also affect the results. For instance, in the SH

significant temperature variations appear to take place mainly in the West Antarctic region, the area where the Antarctic interannual variability has been reported to be largest [see Lachlan-Cope *et al.*, 2001, and references therein].

[22] The empirical analysis performed here does not allow us to identify a mechanism by which geomagnetic activity would affect the SAT. Rozanov *et al.* [2005] suggest that SAT effects follow EPP- $\text{NO}_x$ -catalyzed  $\text{O}_3$  depletion that leads to circulation changes including a stronger polar vortex. We observe the largest changes in the polar region during winter, when the stratospheric  $\text{NO}_x$  catalytic cycle is weak or inoperative, although noncatalytic  $\text{O}_3$  depletion by reaction with EPP-NO will contribute to the changes. If the wintertime ozone changes were significant enough, one possible mechanism connecting the EPP- $\text{NO}_x$  and the changes at surface level could be coupling through planetary wave breaking: Ozone changes could affect stratospheric winds so that breaking of vertically propagating planetary scale Rossby waves from the troposphere would be affected, this breaking could drive the downward propagation of NAM-like patterns which would ultimately be seen in the SAT. The resemblance of the NH  $\Delta\text{SAT}$  patterns to the typical cell-like NAM pattern effects in the meteorological data used here and the similarity of model predictions of Rozanov *et al.* [2005] to the positive NAM SAT pattern perhaps indicates a common mechanism between the NAM and changes induced by geomagnetic variations. The origin of the annular mode patterns is not yet fully understood,

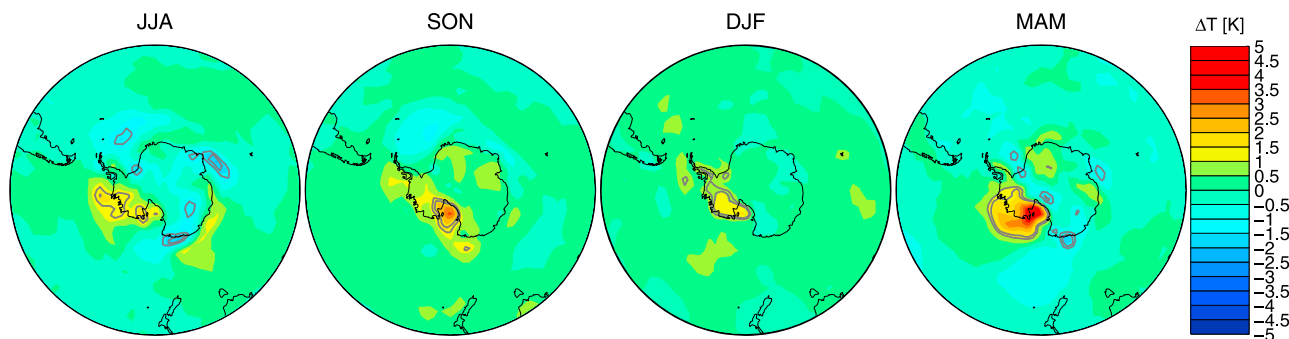


**Figure 10.** Southern hemisphere temperature variability test for random solar flux and  $A_p$  variability (see text for details).



although it is possibly linked to polar vortex strength [Baldwin *et al.*, 2003]. It remains uncertain why the meteorological data implies a stronger surface temperature response than the modeling, but one possible source for the difference could arise from the year-to-year variability in the EPP source and the particle energy limitations of the data set used by Rozanov *et al.* [2005]; The particle data used in the modeling represented a low geomagnetic activity year (1987, see Figure 1) and was for limited energy range only. As separation of atmospheric response for the forcing from different sources will always be challenging from observational data, it would be important to put effort in examining these effects through models including realistic middle and upper atmosphere representation, coupling mechanisms for the atmospheric layers and ever more realistic geomagnetic activity (EPP) sources. Through model work we will be able to look in detail into the mechanisms communicating signatures from high altitudes all the way to the surface level. This presents a future challenge to atmospheric modeling work, but it is equally important to note that in order to be able to reliably model the response from geomagnetic sources we also need better understanding of the different particle sources: This provides a challenge to the scientific community working on solar-terrestrial physics.

[23] If true, the EPP feedback would be complex, since strong vortices lead to large EPP effects due to NO<sub>x</sub> sequestration [Randall *et al.*, 2007], but stratospheric warmings can also be followed by large EPP effects due to enhanced mesospheric descent [Siskind *et al.*, 2007]. However, our analysis suggests that years with SSWs produce weaker correlations between geomagnetic activity and ΔSAT.

[24] **Acknowledgments.** We thank the Academy of Finland for their support for the work of AS through the EPPIC (125336), EPPIC-PR (128648), and THERMES (123275) projects. We are grateful for ECMWF for providing the extended ERA-40 data set. A.S. thanks L. Thölix/FMI for valuable help with ERA-40 and L.V. Harvey/UC for useful conversations. C.E.R. was supported by NASA LWS grant NNX06AC05G. The ERA-40 and ECMWF operational data were available through FMI.

[25] Zuyin Pu thanks the reviewers for their assistance in evaluating this paper.

## References

- Austin, J., et al. (2008), Coupled chemistry climate model simulations of the solar cycle in ozone and temperature, *J. Geophys. Res.*, *113*, D11306, doi:10.1029/2007JD009391.
- Baldwin, M. P., and T. J. Dunkerton (1999), Propagation of the Arctic Oscillation from the stratosphere to the troposphere, *J. Geophys. Res.*, *104*(D24), 30,937–30,946.
- Baldwin, M. P., D. B. Stephenson, D. W. J. Thompson, T. J. Dunkerton, A. J. Charlton, and A. O'Neill (2003), Stratospheric memory and skill of extended-range weather forecasts, *Science*, *301*, 636–640.
- Boberg, F., and H. Lundstedt (2002), Solar wind variations related to fluctuations of the North Atlantic Oscillation, *Geophys. Res. Lett.*, *29*(15), 1718, doi:10.1029/2002GL014903.
- Brasseur, G. P., and S. Solomon (2005), *Aeronomy of the Middle Atmosphere*, 3rd ed., Springer, Dordrecht, Netherlands.
- Hartley, D. E., J. T. Villarin, R. X. Black, and C. A. Davis (1998), A new perspective on the dynamical link between the stratosphere and troposphere, *Nature*, *391*, 471–474.
- Hurrell, J. W., Y. Kushnir, G. Ottersen, and M. Visbeck (Eds.) (2003), *The North Atlantic Oscillation: Climate Significance and Environmental Impact*, *Geophys. Monogr. Ser.*, vol. 134, 279 pp., AGU, Washington, D. C.
- IPCC (2007), *Climate Change 2007 — The Physical Science, Basis Contribution of Working Group I to the Fourth Assessment Report of the IPCC*, Cambridge Univ. Press, Cambridge, U. K.
- Klein Tank, A. M. G., et al. (2002), Daily dataset of 20th-century surface air temperature and precipitation series for the European Climate Assessment, *Int. J. Climatol.*, *22*, 1441–1453.
- Kuroda, Y. (2008), Effect of stratospheric sudden warming and vortex intensification on the tropospheric climate, *J. Geophys. Res.*, *113*, D15110, doi:10.1029/2007JD009550.
- Lachlan-Cope, T. A., W. M. Connolley, and J. Turner (2001), The role of the non-axisymmetric antarctic orography in forcing the observed pattern of variability of the antarctic climate, *Geophys. Res. Lett.*, *28*, 4111–4114.
- Langematz, U., J. L. Grenfell, K. Matthes, P. Mieth, M. Kunze, B. Steil, and C. Brühl (2005), Chemical effects in 11-year solar cycle simulations with the Freie Universität Berlin Climate Middle Atmosphere Model with online chemistry (FUB-CMAM-CHEM), *Geophys. Res. Lett.*, *32*, L13803, doi:10.1029/2005GL022686.
- Lopéz-Puertas, M., B. Funke, S. Gil-Lopéz, T. v. Clarmann, G. P. Stiller, M. Höpfner, S. Kellmann, H. Fischer, and C. H. Jackman (2005), Observation of NO<sub>x</sub> enhancement and ozone depletion in the northern and southern hemispheres after the October–November 2003 solar proton events, *J. Geophys. Res.*, *110*, A09S43, doi:10.1029/2005JA011050.
- Lu, H., M. A. Clilverd, A. Seppälä, and L. L. Hood (2008), Geomagnetic perturbations on stratospheric circulation in late winter and spring, *J. Geophys. Res.*, *113*, D16106, doi:10.1029/2007JD008915.
- Manney, G. L., K. Krüger, J. L. Sabutis, S. A. Sena, and S. Pawson (2005), The remarkable 2003–2004 winter and other recent warm winters in the Arctic stratosphere since the late 1990s, *J. Geophys. Res.*, *110*, D04107, doi:10.1029/2004JD005367.
- Mayaud, P. (1980), *Derivation, Meaning and Use of Geomagnetic Indices*, *Geophys. Monogr. Ser.*, vol. 22, AGU, Washington, D. C.
- Randall, C. E., D. W. Rusch, R. M. Bevilacqua, K. W. Hoppel, and J. D. Lumpe (1998), Polar Ozone and Aerosol Measurement (POAM) II stratospheric NO<sub>2</sub>, 1993–1996, *J. Geophys. Res.*, *103*, 28,361–28,372.
- Randall, C. E., D. E. Siskind, and R. M. Bevilacqua (2001), Stratospheric NO<sub>x</sub> enhancements in the southern hemisphere vortex in winter/spring of 2000, *Geophys. Res. Lett.*, *28*, 2385–2388.
- Randall, C. E., et al. (2005), Stratospheric effects of energetic particle precipitation in 2003–2004, *Geophys. Res. Lett.*, *32*, L05802, doi:10.1029/2004GL022003.
- Randall, C. E., V. L. Harvey, C. S. Singleton, P. F. Bernath, C. D. Boone, and J. U. Kozyra (2006), Enhanced NO<sub>x</sub> in 2006 linked to upper stratospheric Arctic vortex, *Geophys. Res. Lett.*, *33*, L18811, doi:10.1029/2006GL027160.
- Randall, C. E., V. L. Harvey, C. S. Singleton, S. M. Bailey, P. F. Bernath, M. Codrescu, H. Nakajima, and J. M. Russell III (2007), Energetic particle precipitation effects on the Southern Hemisphere stratosphere in 1992–2005, *J. Geophys. Res.*, *112*, D08308, doi:10.1029/2006JD007696.
- Rozanov, E., L. Callis, M. Schlesinger, F. Yang, N. Andronova, and V. Zubov (2005), Atmospheric response to NO<sub>x</sub> source due to energetic electron precipitation, *Geophys. Res. Lett.*, *32*, L14811, doi:10.1029/2005GL023041.
- Seppälä, A., P. T. Verronen, E. Kyrölä, S. Hassinen, L. Backman, A. Hauchecorne, J. L. Bertaux, and D. Fussen (2004), Solar proton events of October–November 2003: Ozone depletion in the Northern hemisphere polar winter as seen by GOMOS/Envisat, *Geophys. Res. Lett.*, *31*, L19107, doi:10.1029/2004GL021042.
- Seppälä, A., P. T. Verronen, M. A. Clilverd, C. E. Randall, J. Tamminen, V. F. Sofieva, L. Backman, and E. Kyrölä (2007), Arctic and Antarctic polar winter NO<sub>x</sub> and energetic particle precipitation in 2002–2006, *Geophys. Res. Lett.*, *34*, L12810, doi:10.1029/2007GL029733.
- Siskind, D. E., G. E. Nedoluha, C. E. Randall, M. Fromm, and J. M. Russell III (2000), An assessment of Southern Hemisphere stratospheric NO<sub>x</sub> enhancements due to transport from the upper atmosphere, *Geophys. Res. Lett.*, *27*, 329–332.
- Siskind, D. E., S. D. Eckermann, L. Coy, J. P. McCormack, and C. E. Randall (2007), On recent interannual variability of the Arctic winter mesosphere: Implications for tracer descent, *Geophys. Res. Lett.*, *34*, L09806, doi:10.1029/2007GL029293.
- Song, Y. C., and W. A. Robinson (2004), Dynamical mechanisms for stratospheric influences on the troposphere, *J. Atmos. Sci.*, *61*(14), 1711–1725.
- Thejll, P., B. Christiansen, and H. Gleisner (2003), On correlations between the North Atlantic Oscillation, geopotential heights, and geomagnetic activity, *Geophys. Res. Lett.*, *30*(6), 1347, doi:10.1029/2002GL016598.
- Thompson, D. W. J., and J. M. Wallace (2000), Annular modes in the extratropical circulation: Part I. Month-to-month variability, *J. Clim.*, *13*, 1000–1016.
- Turner, J., J. C. Comiso, G. J. Marshall, T. A. Lachlan-Cope, T. Bracegirdle, T. Maksym, M. P. Meredith, Z. Wang, and A. Orr (2009), Non-annular atmospheric circulation change induced by stratospheric ozone depletion

and its role in the recent increase of Antarctic sea ice extent, *Geophys. Res. Lett.*, 36, L08502, doi:10.1029/2009GL037524.  
Uppala, S. M., et al. (2005), The ERA-40 re-analysis, *Q. J. R. Meteorol. Soc.*, 131, 2961–3012, doi:10.1256/qj.04.176.

---

M. A. Clilverd, British Antarctic Survey (NERC), High Cross, Madingley Road, Cambridge CB3 0ET, UK.

C. E. Randall, Laboratory for Atmospheric and Space Physics and Department of Atmospheric and Oceanic Sciences, University of Colorado, 392 UCB, Boulder, CO 80309-0392, USA.

C. J. Rodger, Department of Physics, University of Otago, P.O. Box 56, 9054 Dunedin, New Zealand.

E. Rozanov, Physical-Meteorological Observatory/World Radiation Center, CH-7260 Davos, Switzerland.

A. Seppälä, Finnish Meteorological Institute, P.O. Box 503, FI-00101 Helsinki, Finland. (annika.seppala@fmi.fi)